CHAPTER 4
PROPERTIES OF ROCK MATERIALS

Rock material is the intact rock portion. This Chapter addresses properties of rock material.

4.1 Physical Properties of Rock Material

4.1.1 Density, Porosity and Water Content

Density is a measure of mass per unit of volume. Density of rock material various, and often related to the porosity of the rock. It is sometimes defined by unit weight and specific gravity. Most rocks have density between 2,500nd 2,800 kg/m^3.

Porosity describes how densely the material is packed. It is the ratio of the non-solid volume to the total volume of material. Porosity therefore is a fraction between 0 and 1. The value is typically ranging from less than 0.01 for solid granite to up to 0.5 for porous sandstone. It may also be represented in percent terms by multiplying the fraction by 100%.

Water content is a measure indicating the amount of water the rock material contains. It is simply the ratio of the volume of water to the bulk volume of the rock material.

Density is common physical properties. It is influenced by the specific gravity of the composition minerals and the compaction of the minerals. However, most rocks are well compacted and then have specific gravity between 2.5 to 2.8. Density is used to estimate overburden stress.

Density and porosity often related to the strength of rock material. A low density and high porosity rock usually has low strength.

Porosity is one of the governing factors for the permeability. Porosity provides the void for water to flow through in a rock material. High porosity therefore naturally leads to high permeability.

Table 4.1.1a gives common physical properties, including density and porosity of rock materials.

Table 4.1.1a Physical properties of fresh rock materials.

Rock	Dry Density (g/cm^3)	Porosity (%)	Schmidt Hardness Index	Cerchar Abrasivitiy Index	P-Wave Velocity (m/s)	S-Wave Velocity (m/s)	Coefficient of Permeability (m/s)
Igneous							
Granite	2.53 – 2.62	1.02 – 2.87	54 – 69	4.5 – 5.3	4500 – 6500	3500 – 3800	10^{-14} – 10^{-12}
Diorite	2.80 – 3.00	0.10 – 0.50		4.2 – 5.0	4500 – 6700		10^{-14} – 10^{-12}
Gabbro	2.72 – 3.00	1.00 – 3.57		3.7 – 4.6	4500 – 7000		10^{-14} – 10^{-12}
Rhyolite	2.40 – 2.60	0.40 – 4.00					10^{-14} – 10^{-12}
Andesite	2.50 – 2.80	0.20 – 8.00	67	2.7 – 3.8	4500 – 6500		10^{-14} – 10^{-12}
Basalt	2.21 – 2.77	0.22 – 22.1	61	2.0 – 3.5	5000 – 7000	3660 – 3700	10^{-14} – 10^{-12}
Sedimentary							
Conglomerate	2.47 – 2.76			1.5 – 3.8			10^{-10} – 10^{-8}
Sandstone	1.91 – 2.58	1.62 – 26.4	10 – 37	1.5 – 4.2	1500 – 4600		10^{-10} – 10^{-8}
Shale	2.00 – 2.40	20.0 – 50.0		0.6 – 1.8	2000 – 4600		
Mudstone	1.82 – 2.72		27				10^{-11} – 10^{-9}
Dolomite	2.20 – 2.70	0.20 – 4.00			5500		10^{-12} – 10^{-11}
Limestone	2.67 – 2.72	0.27 – 4.10	35 – 51	1.0 – 2.5	3500 – 6500		10^{-13} – 10^{-10}
Metamorphic							
Gneiss	2.61 – 3.12	0.32 – 1.16	49	3.5 – 5.3	5000 – 7500		10^{-14} – 10^{-12}
Schist	2.60 – 2.85	10.0 – 30.0	31	2.2 – 4.5	6100 – 6700	3460 – 4000	10^{-11} – 10^{-8}
Phyllite	2.18 – 3.30						
Slate	2.71 – 2.78	1.84 – 3.64		2.3 – 4.2	3500 – 4500		10^{-14} – 10^{-12}
Marble	2.51 – 2.86	0.65 – 0.81			5000 – 6000		10^{-14} – 10^{-11}
Quartzite	2.61 – 2.67	0.40 – 0.65		4.3 – 5.9			10^{-14} – 10^{-13}

4.1.2 Hardness

Hardness is the characteristic of a solid material expressing its resistance to permanent deformation. Hardness of a rock materials depends on several factors, including mineral composition and density. A typical measure is the Schmidt rebound hardness number.

4.1.3 Abrasivity

Abrasivity measures the abrasiveness of a rock materials against other materials, e.g., steel. It is an important measure for estimate wear of rock drilling and boring equipment.

Abrasivity is highly influenced by the amount of quartz mineral in the rock material. The higher quartz content gives higher abrasivity.

Abrasivity measures are given by several tests. Cerchar and other abrasivity tests are described later.

4.1.4 Permeability

Permeability is a measure of the ability of a material to transmit fluids. Most rocks, including igneous, metamorphic and chemical sedimentary rocks, generally have very low permeability. As discussed earlier, permeability of rock material is governed by porosity. Porous rocks such as sandstones usually have high permeability while granites have low permeability. Permeability of rock materials, except for those porous one, has limited interests as in the rock mass, flow is concentrated in fractures in the rock mass. Permeability of rock fractures is discussed later.

4.1.5 Wave Velocity

Measurements of wave are often done by using P wave and sometimes, S waves. P-wave velocity measures the travel speed of longitudinal (primary) wave in the material, while S-wave velocity measures the travel speed of shear (secondary) wave in the material. The velocity measurements provide correlation to physical properties in terms of compaction degree of the material. A well compacted rock has generally high velocity as the grains are all in good contact and wave are travelling through the solid. For a poorly compact rock material, the grains are not in good contact, so the wave will partially travel through void (air or water) and the velocity will be reduced (P-wave velocities in air and in water are 340 and 1500 m/s respectively and are much lower than that in solid). Typical values of P and S wave velocities of some rocks are given in Table 4.1.1a. Wave velocities are also commonly used to assess the degree of rock mass fracturing at large scale, using the same principle, and it will be discussed in a later chapter.

4.2 Mechanical Properties of Rock Material

4.2.1 Compressive Strength

Compressive strength is the capacity of a material to withstand axially directed compressive forces. The most common measure of compressive strength is the uniaxial compressive strength or unconfined compressive strength. Usually compressive strength of rock is defined by the ultimate stress. It is one of the most important mechanical properties of rock material, used in design, analysis and modelling.

Figure 4.2.1a presents a typical stress-strain curve of a rock under uniaxial compression. The complete stress-strain curve can be divided into 6 sections, represent 6 stages that the rock material is undergoing. Figure 4.2.1b and Figure 4.2.1c show the states of rock in those stages of compression.

Figure 4.2.1a Typical uniaxial compression stress-strain curve of rock material.

Figure 4.2.1b Uniaxial compression test and failure simulated by RFPA.

Figure 4.2.1c Samples of rock material under uniaxial compression test and failure.

Stage I – The rock is initially stressed, pre-existing microcracks or pore orientated at large angles to the applied stress is closing, in addition to deformation. This causes an initial non-linearity of the axial stress-strain curve. This initial non-linearity is more obvious in weaker and more porous rocks,

Stage II – The rock basically has a linearly elastic behaviour with linear stress-strain curves, both axially and laterally. The Poisson's ratio, particularly in stiffer unconfined rocks, tends to be low. The rock is primarily undergoing elastic deformation with minimum cracking inside the material. Micro-cracks are likely initiated at the later portion of this stage, of about 35-40% peak strength. At this stage, the stress-strain is largely recoverable, as the there is little permanent damage of the micro-structure of the rock material.

Stage III – The rock behaves near-linear elastic. The axial stress-strain curve is near-linear and is nearly recoverable. There is a slight increase in lateral strain due to dilation. Microcrack propagation occurs in a stable manner during this stage and that microcracking events occur independently of each other and are distributed throughout the specimen. The upper boundary of the stage is the point of maximum compaction and zero volume change and occurs at about 80% peak strength.

Stage IV – The rock is undergone a rapid acceleration of microcracking events and volume increase. The spreading of microcracks is no longer independent and clusters of cracks in the zones of highest stress tend to coalesce and start to form tensile fractures or shear planes - depending on the strength of the rock.

Stage V – The rock has passed peak stress, but is still intact, even though the internal structure is highly disrupt. In this stage the crack arrays fork and coalesce into macrocracks or fractures. The specimen is undergone strain softening (failure) deformation, i.e., at peak stress the test specimen starts to become weaker with increasing strain. Thus further strain will be concentrated on weaker elements of the rock which have already been subjected to strain. This in turn will lead to zones of concentrated strain or shear planes.

Stage VI – The rock has essentially parted to form a series of blocks rather than an intact structure. These blocks slide across each other and the predominant deformation mechanism is friction between the sliding blocks. Secondary fractures may occur due to differential shearing. The axial stress or force acting on the specimen tends to fall to a constant residual strength value, equivalent to the frictional resistance of the sliding blocks.

In underground excavation, we often are interested in the rock at depth. The rock is covered by overburden materials, and is subjected to lateral stresses. Compressive strength with lateral pressures is higher than that without. The compressive strength with lateral pressures is called triaxial compressive strength. The true triaxial compression means the 3 different principal stresses in three directions. A true triaxial compression testing machine is rather difficult to operate. In most tests, two lateral stresses are made equal, i.e., $\sigma_2 = \sigma_3$. In the test, only a confining pressure is required.

Figure 4.2.1d shows the results of a series triaxial compression tests. In addition to the significant increase of strength with confining pressure, the stress-strain characteristics also changed. Discussion on the influence of confining pressure to the mechanical characteristics is given in a later section. Typical strengths and modulus of common rocks are given in Table 4.2.1a.

Figure 4.2.1d Triaxial compression test and failure

Table 4.2.1a Mechanical properties of rock materials.

Rock	UC Strength (MPa)	Tensile Strength (MPa)	Elastic Modulus (GPa)	Poisson's Ratio	Strain at Failure (%)	Point Load Index $I_{s(50)}$ (MPa)	Fracture Mode I Toughness
Igneous							
Granite	100 – 300	7 – 25	30 – 70	0.17	0.25	5 – 15	0.11 – 0.41
Dolerite	100 – 350	7 – 30	30 – 100	0.10 – 0.20	0.30		>0.41
Gabbro	150 – 250	7 – 30	40 – 100	0.20 – 0.35	0.30	6 – 15	>0.41
Rhyolite	80 – 160	5 – 10	10 – 50	0.2 – 0.4			
Andesite	100 – 300	5 – 15	10 – 70	0.2		10 – 15	
Basalt	100 – 350	10 – 30	40 – 80	0.1 – 0.2	0.35	9 – 15	>0.41
Sedimentary							
Conglomerate	30 – 230	3 – 10	10 – 90	0.10 – 0.15	0.16		
Sandstone	20 – 170	4 – 25	15 – 50	0.14	0.20	1 – 8	0.027 – 0.041
Shale	5 – 100	2 – 10	5 – 30	0.10			0.027 – 0.041
Mudstone	10 – 100	5 – 30	5 – 70	0.15	0.15	0.1 – 6	
Dolomite	20 – 120	6 – 15	30 – 70	0.15	0.17		
Limestone	30 – 250	6 – 25	20 – 70	0.30		3 – 7	0.027 – 0.041
Metamorphic							
Gneiss	100 – 250	7 – 20	30 – 80	0.24	0.12	5 – 15	0.11 – 0.41
Schist	70 – 150	4 – 10	5 – 60	0.15 – 0.25		5 – 10	0.005 – 0.027
Phyllite	5 – 150	6 – 20	10 – 85	0.26			
Slate	50 – 180	7 – 20	20 – 90	0.20 – 0.30	0.35	1 – 9	0.027 – 0.041
Marble	50 – 200	7 – 20	30 – 70	0.15 – 0.30	0.40	4 – 12	0.11 – 0.41
Quartzite	150 – 300	5 – 20	50 – 90	0.17	0.20	5 – 15	>0.41

4.2.2 Young's Modulus and Poisson's Ratio

Young's Modulus is modulus of elasticity measuring of the stiffness of a rock material. It is defined as the ratio, for small strains, of the rate of change of stress with strain. This can be experimentally determined from the slope of a stress-strain curve obtained during compressional or tensile tests conducted on a rock sample.

Similar to strength, Young's Modulus of rock materials varies widely with rock type. For extremely hard and strong rocks, Young's Modulus can be as high as 100 GPa. There is some correlation between compressive strength and Young's Modulus, and discussion is given in a later section.

Poisson's ratio measures the ratio of lateral strain to axial strain, at linearly-elastic region. For most rocks, the Poisson's ratio is between 0.15 and 0.4. As seen from early section, at later stage of loading beyond linearly elastic region, lateral strain increase fast than the axial strain and hence lead to a higher ratio.

4.2.3 Stress-Strain at and after Peak

With well controlled compression test, a complete stress-strain curve for a rock specimen can be obtained, as typically shown in Figure 4.2.3a.

Figure 4.2.3a Complete stress-strain curves of several rocks showing post peak behaviour (Brady and Brown).

Strain at failure is the strain measured at ultimate stress. Rocks generally fail at a small strain, typically around 0.2 to 0.4% under uniaxial compression. Brittle rocks, typically crystalline rocks, have low strain at failure, while soft rock, such as shale and mudstone, could have relatively high strain at failure. Strain at failure sometimes is used as a measure of brittleness of the rock. Strain at failure increases with increasing confining pressure under triaxial compression conditions.

Rocks can have brittle or ductile behaviour after peak. Most rocks, including all crystalline igneous, metamorphic and sedimentary rocks, behave brittle under uniaxial compression. A few soft rocks, mainly of sedimentary origin, behave ductile.

4.2.4 Tensile Strength

Tensile strength of rock material is normally defined by the ultimate strength in tension, i.e., maximum tensile stress the rock material can withstand.

Rock material generally has a low tensile strength. The low tensile strength is due to the existence of microcracks in the rock. The existence of microcracks may also be the cause of rock failing suddenly in tension with a small strain.

Tensile strength of rock materials can be obtained from several types of tensile tests: direct tensile test, Brazilian test and flexure test. Direct test is not commonly performed due to the difficulty in sample preparation. The most common tensile strength determination is by the Brazilian tests. Figure 4.2.4a illustrates the failure mechanism of the Brazilian tensile tests.

Figure 4.2.4a Stress and failure of Brazilian tensile tests by RFPA simulation.

4.2.5 Shear Strength

Shear strength is used to describe the strength of rock materials, to resist deformation due to shear stress. Rock resists shear stress by two internal mechanisms, cohesion and internal friction. Cohesion is a measure of internal bonding of the rock material. Internal friction is caused by contact between particles, and is defined by the internal friction angle, ϕ. Different rocks have different cohesions and different friction angles.

Shear strength of rock material ca be determined by direct shear test and by triaxial compression tests. In practice, the later methods is widely used and accepted.

With a series of triaxial tests conducted at different confining pressures, peak stresses (σ_1) are obtained at various lateral stresses (σ_3). By plotting Mohr circles, the shear envelope is defined which gives the cohesion and internal friction angle, as shown in Figure 4.2.5a.

Figure 4.2.5a Determination of shear strength by triaxial tests.

Tensile and shear strengths are important as rock fails mostly in tension and in shearing, even the loading may appears to be compression. Rocks generally have high compressive strength so failure in pure compression is not common.

4.3 Effects of Confining and Pore Water Pressures on Strength and Deformation

4.3.1 Effects of Confining Pressure

Figure 4.3.1a illustrates a number of important features of the behaviour of rock in triaxial compression. It shows that with increasing confining pressure,

(a) the peak strength increases;

(b) there is a transition from typically brittle to fully ductile behaviour with the introduction of plastic mechanism of deformation;
(c) the region incorporating the peak of the axial stress-axial strain curve flattens and widens;
(d) the post-peak drop in stress to the residual strength reduces and disappears at high confining stress.

Figure 4.3.1a Complete axial stress-axial strain curves obtained in triaxial compression tests on Tennessee Marble at various confining pressures (after Wawersik & Fairhurst 1970).

The confining pressure that causes the post-peak reduction in strength disappears and the behaviour becomes fully ductile (48.3 MPa in the figure), is known as the brittle-ductile transition pressure. This brittle-ductile transition pressure varies with rock type. In general, igneous and high grade metamorphic rocks, e.g., granite and quartzite, remain brittle at room temperature at confining pressures of up to 1000 MPa or more. In these cases, ductile behaviour will not be of concern in practical civil engineering problems.

4.3.2 Effects of Pore Water Pressure

The influence of pore-water pressure on the behaviour of porous rock in the triaxial compression tests is illustrated by Figure 4.3.2a. A series of triaxial compression tests was carried out on a limestone with a constant confining pressure of 69 MPa, but with various level of pore pressure (0-69 MPa). There is a transition from ductile to brittle behaviour as pore pressure is increased from 0 to 69 MPa. In this case, mechanical response is controlled by the effective confining stress ($\sigma_3' = \sigma_3 - u$).

Figure 4.3.2a Effect of pore pressure on the stress-strain behaviour of rock materials.

Effect of pore water pressure is only applicable for porous rocks where sufficient pore pressure can be developed within the materials. For low porosity rocks, the classical effective stress law does not hold.

4.3.3 Effects of Intermediate Stress

The axisymmetric triaxial test is a simplified method to determine the axial strength at a confining pressure. The effect of intermediate principal stress (σ_2) is not considered. Under the true triaxial compression condition ($\sigma_2 > \sigma_3$), it is found that σ_2 has effects on the axial strength. Figure 4.3.3a shows some typical results of the true triaxial test on granite and marble (Mogi, Yu).

Figure 4.3.3a Change of triaxial compressive strength with intermediate principal stress.

It is evident that rock triaxial compressive strength increases with σ_2 with a fixed σ_3. This is a conclusion quite different from the conventional Mohr-Coulomb strength criterion. It is further suggested that the σ_2 effect have two zones: (i) rock triaxial compressive strength increases with increasing σ_2 from $\sigma_2 = \sigma_3$ to a critical value (σ_2'); and (ii) rock triaxial compressive strength decreases with further increasing of σ_2 from $\sigma_2 = \sigma_2'$ to $\sigma_2 = \sigma_1$, as shown in Figure 4.3.3b.

Figure 4.3.3b Effect of intermediate stress on peak strength.

Within the practical range of civil engineering, σ_2 and σ_3 will generally significant small compare to the strength. Having $\sigma_2 = \sigma_3$, tests give a slightly lower and more conservative estimate of the strength. However, in petroleum engineering applications, the engineering depths could reach a few thousands meters, the effect of σ_2 on the estimation of strength could be significant in engineering design.

4.4 Other Engineering Properties of Rock Materials

4.4.1 Point Load Strength Index

Point load test is another simple index test for rock material. It gives the standard point load index, $I_{s(50)}$, calculated from the point load at failure and the size of the specimen, with size correction to an equivalent core diameter of 50 mm. Description of point load test and calculation is given later in the section dealing with laboratory test methods.

Typical values of point load strength index for various rocks are given in Table 4.2.1a.

4.4.2 Fracture Toughness

Fracture toughness of rock materials measures the effectiveness of rock fracturing. It is typically measured by a toughness test. There are three fracture mode: (Mode I), (Mode II) (Mode III), as shown in Figure 4.4.2a. Correspondingly, there are three fracture toughness, K_{IC}, K_{IIC} and K_{IIIC}.

Figure 4.4.2a Three typical fracture modes.

In rock mechanics, Mode I is associated with the crack initiation and propagation in a rock material. Table 4.2.1a gives values of K_{IC} for typical rocks.

4.4.3 Brittleness

Brittleness can be expressed by several ways.

4.4.4 Indentation

4.4.5 Swelling

Some rocks swell when they are situated with water. As discussed in Chapter 2, swelling is governed by the amount of swelling montmorillonite clay minerals in the rock material.

Rock swelling is measured in confined and unconfined conditions. Unconfined swelling is measured by the percentage increase of length in three perpendicular directions, when a rock specimen is placed in water.

Confined swelling index measures swelling in one direction while deformations in other two directions are constrained.

4.5 Relationships between Physical and Mechanical Properties

4.5.1 Rock Hardness, Density, and Strength

Schmidt hammer rebound hardness is often measured during early part of field investigation. It is a measure of the hardness of the rock material by count the rebound degree. At the same time, the hardness index can be used to estimate uniaxial compressive strength of the rock material. The correlation between hardness and strength is shown in Figure 4.5.1a. The correlation is also influenced by the density of the material.

Figure 4.5.1a Correlation between hardness, density and strength.

4.5.2 Effect of Water Content on Strength

Many tests showed that the when rock materials are saturated or in wet condition, the uniaxial compressive strength is reduced, compared to the strength in dry condition.

4.5.3 Velocity and Modulus

While seismic wave velocity gives a physical measurement of the rock material, it is also used to estimate the elastic modulus of the rock material. From the theory of elasticity, compressional (or longitudinal) P-wave velocity (v_p) is related to the elastic modulus (E_s), and the density (ρ) of the material as,

$$v_p = (E_s / \rho)^{½} \qquad \text{or} \qquad E_s = \rho\, v_p^2$$

If ρ in g/cm^3, and v_p in km/s, then E_s in GPa (10^9 N/m^2). The elastic modulus estimated by this method is the sometime termed as seismic modulus (also called dynamic modulus, but should not be mistaken as the modulus under dynamic compression). It is different from the modules obtained by the uniaxial compression tests. The value of the seismic modulus is generally slightly higher than the modulus determined from static compression tests.

Similarly, seismic shear modulus G_s may be determined from shear S-wave velocity v_s,

$$G_s = \rho\, v_s^2$$

G_s is in GPa, when density ρ is in g/cm^3, and S-wave velocity v_s is in km/s. Seismic Poisson's ration ν_s can be determined from,

$$\nu_s = \frac{1 - 2\,(v_s / v_p)^2}{2\,[1 - (v_s / v_p)^2]}$$

Alternatively, seismic Young's modulus E_s can be determined from shear modulus (G_s) and Poisson's ratio (ν_s),

$$E_s = 2\, G_s\, (1 + \nu_s)$$

4.5.4 Compressive Strength and Modulus

It is a general trend that a stronger rock material is also stiffer, i.e., higher elastic modulus is often associated with higher strength. There is reasonable correlation between compressive strength and elastic modulus. The correlations are presented in Figure 4.5.4a.

Figure 4.5.4a Correlation between strength and modulus.

It should be noted that the correlation is not precisely linear and also depends on the rock type, or perhaps on the texture of the rocks.

4.5.5 Compressive and Tensile Strengths

As shown by the Griffith criterion, tensile strength of brittle materials is theoretical 1/8 of the compressive strength. Typically, tensile strength of rock materials is about 1/10 to 1/8 of the compressive strength.

It is important to be aware that compressive strength is significantly greater than tensile strength for rocks. Therefore, rock fails easily under tension. In design, rock should be subjected to minimum tensile stress.

4.5.6 Point Load Index and Strengths

With massive tests results, correlations between the point load index ($I_{s(50)}$)and uniaxial compressive strength (σ_c)and between the point load index and Brazilian tensile strength (σ_t)are suggested as below,

$\sigma_c \approx 22\ I_{s(50)}$
$\sigma_t \approx 1.25\ I_{s(50)}$

However, it is noted the correlation factor between σ_c and $I_{s(50)}$ can vary between 10 to 30. By theoretical analysis, the correlation factor is 12.5 (Chua and Wong 1996). It is strongly suggested that the point load index should be used as an independent strength index, and should not used to determine the compressive strength.

The correlation between σ_t and $I_{s(50)}$ is more consistent, and again, it can vary with a significant margin. The failure mode for point load test is primarily by tensile fracturing.

4.5.7 Point Load Index and Fracture Toughness

As the point load failure is due to Mode I fracturing, it is therefore anticipated some correlations between Mode I Fracture Toughness (K_{IC}) and point load index ($I_{s(50)}$). Two correlations below are suggested based on test results,

$K_{IC} \approx 1.1 + 0.1\ I_{s(50)}$

$K_{IC} \approx 0.21\ I_{s(50)}$

The first equation gives a higher estimate at $I_{s(50)}<10$, and lower estimate at $I_{s(50)}>10$, than those of the second equation. When $I_{s(50)} \approx 10$ (typically for crystalline rocks), both correlation equations give $K_{IC} \approx 2.1$.

4.6 Failure Criteria of Rock Materials

4.6.1 Mohr-Coulomb criterion

Mohr-Coulomb strength criterion assumes that a shear failure plane is developed in the rock material. When failure occurs, the stresses developed on the failure plane are on the strength envelope. Refer to Figure 4.6.1a, the stresses on the failure plane a-b are the normal stress σ_n and shear stress τ.

Figure 4.6.1a Stresses on failure plane a-b and representation of Mohr's circle.

Applying the stress transformation equations or from the Mohr's circle, it gives:

$$\sigma_n = \tfrac{1}{2} (\sigma_1 + \sigma_3) + \tfrac{1}{2} (\sigma_1 - \sigma_3) \cos 2\theta$$

$$\tau = \tfrac{1}{2} (\sigma_1 - \sigma_3) \sin 2\theta$$

Coulomb suggested that shear strengths of rock are made up of two parts, a constant cohesion (c) and a normal stress-dependent frictional component, i.e.,

$$\tau = c + \sigma_n \tan\phi$$

where c = cohesion and ϕ = angle of internal friction.

Therefore, by combining the above three equations,

$$\tfrac{1}{2} (\sigma_1 - \sigma_3) \sin 2\theta = c + [\tfrac{1}{2} (\sigma_1 + \sigma_3) + \tfrac{1}{2} (\sigma_1 - \sigma_3) \cos 2\theta] \tan\phi$$

or

$$\sigma_1 = \frac{2c + \sigma_3 [\sin 2\theta + \tan\phi (1 - \cos 2\theta)]}{\sin 2\theta - \tan\phi (1 + \cos 2\theta)}$$

In a shear stress-normal stress plot, the Coulomb shear strength criterion $\tau = c + \sigma_n \tan\phi$ is represented by a straight line, with an intercept c on the τ axis and an angle of ϕ with the σ_n axis. This straight line is often called the strength envelope. Any stress condition below the strength envelope is safe, and once the stress condition meet the envelope, failure will occur.

As assumed, rock failure starts with the formation of the shear failure plane a-b. Therefore, the stress condition on the a-b plane satisfies the shear strength condition. In another word, the Mohr-Coulomb strength envelope straight line touches (makes a tangent) to the Mohr's circles. At each tangent point, the stress condition on the a-b plane meets the strength envelope.

As seen from the Mohr's circle, the failure plane is defined by θ, and

$$\theta = \tfrac{1}{4}\,\pi + \tfrac{1}{2}\,\phi$$

Then

$$\sigma_1 = \frac{2c\cos\phi + \sigma_3\,(1+\sin\phi)]}{1-\sin\phi}$$

Figure 4.6.1b Mohr-Coulomb strength envelope in terms of normal and shear stresses and principal stresses, with tensile cut-off.

If the Mohr-Coulomb strength envelope shown in Figure 4.6.1b is extrapolated, the uniaxial compressive strength is related to c and ϕ by:

$$\sigma_c = \frac{2\,c\cos\phi}{1-\sin\phi}$$

An apparent value of uniaxial tensile strength of the material is given by:

$$\sigma_t = \frac{2\,c\cos\phi}{1+\sin\phi}$$

However, the measured values of tensile strength are generally lower than those predicted by the above equation. For this reason, a tensile cut-off is usually applied at a selected value of uniaxial tensile stress, σ_t', as shown in Figure 4.6.1b. For most rocks, σ_t' is about 1/10 σ_c.

The Mohr-Coulomb strength envelope can also be shown in σ_1–σ_3 plots, as seen in Figure 4.6.1b. Then,

$$\sigma_1 = \sigma_c + \sigma_3 \tan\psi$$

and

$$\tan\psi = \frac{1+\sin\phi}{1-\sin\phi}$$

or

$$\sigma_1 = \sigma_c + \sigma_3 \frac{1 + \sin\phi}{1 - \sin\phi}$$

The Mohr-Coulomb criterion is only suitable for the low range of σ_3. At high σ_3, it overestimates the strength. It also overestimates tensile strength. In most cases, rock engineering deals with shallow problems and low σ_3, so the criterion is widely used, due to its simplicity and popularity.

4.6.2 Griffith strength criterion

Based on the energy instability concept, Griffith extended the theory to the case of applied compressive stresses. Assuming that the elliptical crack will propagate from the points of maximum tensile stress concentration (P in Figure 4.6.2a), Griffith obtained the following criterion for crack extension in plane compression:

Figure 4.6.2a Griffith crack model for plane compression.

$$(\sigma_1 - \sigma_3)^2 - 8\,\sigma_t\,(\sigma_1 + \sigma_3) = 0 \qquad \text{if} \qquad \sigma_1 + 3\,\sigma_3 > 0$$

$$\sigma_1 + \sigma_t = 0 \qquad \text{if} \qquad \sigma_1 + 3\,\sigma_3 < 0$$

where σ_t is the uniaxial tensile strength of the material.

When $\sigma_3 = 0$, the above equation becomes

$$\sigma_1 - 8\,\sigma_t = 0$$

It in fact suggests that the uniaxial compressive stress at crack extension is always eight times the uniaxial tensile strength

Figure 4.6.2b Griffith envelope for crack extension in compression.

The strength envelopes given by the above equations in principal stresses and in normal and shear stresses are shown in Figure 4.6.2b. This criterion can also be expressed in terms of the shear stress (τ) and normal stress (σ_n) acting on the plane containing the major axis of the crack:

$$\tau^2 = 4\,\sigma_t\,(\sigma_n + \sigma_t)$$

When $\sigma_n = 0$, $\tau = 2\sigma_t$, which represents the cohesion.

The classic plane compression Griffith theory did not provide a very good model for the peak strength of rock under multiaxial compression. It gives only good estimate of tensile strength, and under-estimate compressive strength. Accordingly, a number of modifications to Griffith's solution were introduced. These criteria do not find practical use today.

4.6.3 Hoek-Brown criterion

Because the classic strength theories used for other engineering materials have been found not to apply to rock over a wide range of applied compressive stress conditions, a number of empirical strength criteria have been introduced for practical use. One of the most widely used criteria is Hoek-Brown criterion for isotropic rock materials and rock masses.

Hoek and Brown (1980) found that the peak triaxial compressive strengths of a wide range of isotropic rock materials could be described by the following equation:

$$\frac{\sigma_1}{\sigma_c} = \frac{\sigma_3}{\sigma_c} + \left(m \frac{\sigma_3}{\sigma_c} + 1.0 \right)^{1/2}$$

or

$$\sigma_1 = \sigma_3 + (m\, \sigma_3\, \sigma_c + \sigma_c^2)^{1/2}$$

Where m is a parameter that changes with rock type in the following general way:

(a) $m \approx 7$ for carbonate rocks with well developed crystal cleavage (dolomite, limestone, marble);
(b) $m \approx 10$ for lithified argillaceous rocks (mudstone, siltstone, shale, slate);
(c) $m \approx 15$ for arenaceous rocks with strong crystals and poorly developed crystal cleavage (sandstaone, quartzite);
(d) $m \approx 17$ for fine-grained polyminerallic igneous crystalline rocks (andesite, dolerite, diabase, rhyolite);
(e) $m \approx 25$ for coarse-grained polyminerallic igneous and metamorphic rocks (amphibolite, gabbro, gneiss, granite, norite, quartz-diorite).

Figure 4.6.3a shows normalized Hoek-Brown peak strength envelope for some rocks. It is evident that the Hoek-Brown strength envelope is not a straight line, but a curve. At high stress level, the envelope curves down, so it gives low strength estimate than the Mohr-Coulomb envelope.

Figure 4.6.3a Normalized peak strength envelope for (i) granites and (ii) sandstones (after Hoek & Brown 1980).

The Hoek-Brown peak strength criterion is an empirical criterion based on substantial test results on various rocks. It is however very easy to use and select parameters. It is also extended to rock masses with the same equation, hence makes it is so far the only acceptable criterion for both material and mass. The Hoek Brown rock mass strength criterion is covered in a later chapter.

4.7 Effects of Rock Microstructures on Mechanical Properties

4.7.1 Strength of rock material with Anisotropy

Rocks, such as shale and slate, are not isotropic. Because of some preferred orientation of fabric or microstructure, or the presence of bedding or cleavage planes, the behaviour of those rocks is anisotropic. There are several forms of anisotropy with various degrees of complexity. It is therefore only the simplest form of anisotropy, transverse isotropy, to be discussed here.

The peak strengths developed by transversely isotropic rocks in triaxial compression vary with the orientation of the plane of isotropy, plane of weakness or foliation plane, with respect to the principal stress directions. Figure 4.7.1a shows some measured variations in peak principal stress difference with the angle of inclination of the major principal stress to the plane of weakness.

Figure 4.7.1a Variation of differential stresses with the inclination angle of the plane of weakness (see Brady & Brown 1985).

Analytical solution shows that principal stress difference (σ_1–σ_3) of a transversely isotropic specimen under triaxial compression shown in Figure 4.7.1a can be given by the equation below (Brady & Brown 1985):

$$(\sigma_1 - \sigma_3) = \frac{2\,(c_w + \sigma_3 \tan\phi_w)}{(1 - \tan\phi_w \cot\beta)\,\sin 2\beta}$$

where c_w = cohesion of the plane of weakness;
ϕ_w = angle of friction of the plane;
β = inclination of the plane.

The minimum strength occurs when

$\tan 2\beta = -\cot \phi_w$, or $\beta = 45° + ½\,\phi_w$

The corresponding value of principal stress difference is,

$$(\sigma_1 - \sigma_3)_{min} = 2\,(c_w + \sigma_3 \tan\phi_w)\,[(1 + \tan^2\phi_w)^{½} + \tan\phi_w]$$

Figure 4.7.1b shows variation of σ_1 at constant σ_3 with angle β, plotted using the above equation. When the weakness plane is at an angle of $45° + ½\,\phi_w$, the strength is the lowest. For rocks, ϕ_w is about 30° to 50°, hence β is about 60° to 70°. In compression tests, intact rock specimens generally fails to form a shear plane at an angle about 60° to 70°. This in fact shows that when the rock containing an existing weakness plane that is about to become a failure plane, the rock has the lowest strength.

Figure 4.7.1b Variation of σ_1 at constant σ_3 with angle β.

4.7.2 Rocks containing Pores and Bridged Cracks

4.7.3 Effects of Mineral Bounding on Rock Material Strength

4.7.4 Effects of Rock Texture Inhomogeneity on Strength and Failure

4.7.5 Soft and Weathered Rocks

Rocks whose uniaxial compressive strength falls approximately in the range 0.5-25 MPa as suggested by ISRM is considered as soft rocks or weak rocks. Soft rocks are usually sediments in the process of consolidation and solidification. Soft or weak rocks can also be weathered rocks.

Soft rocks may have the isotropic compression response similar in detail to the response of consolidated soils, as presented in Figure 4.7.5a. Reader should refer to a soil mechanics textbook for details regarding compressibility.

Figure 4.7.5a Compression characteristics of a soil and a mudstone (Johnston 1993).

The results obtained on over-consolidated London clay showed that for low confining pressures, the stress-strain behaviour is relative brittle. As the confining pressure was increased, the response became more ductile. Exactly the same responses are displayed for soft rocks, and indeed for hard rocks.

The behaviour of soft rocks is somewhere between soil and hard rock. For soil, strength criterion is generally represented by the Mohr-Coulomb criterion, while for hard rocks, it is by the Hoek-Brown criterion. The former is a straight line and the later is a curve.

The strength characteristics of soft rocks are somehow, between soil and hard rock and are described by parabolic curves shown in Figure 4.7.5b.

Figure 4.7.5b Strength envelopes of soils, soft rocks and hard rocks (Johnston 1993).

With increase of strength of geomaterials, there is a general progression from the linear strength criterion of Mohr-Coulomb for soft soil to the curved strength criterion of Hoek-Brown for competent rocks. A criterion describing this progression is given by Johnston (1993) as,

$$\frac{\sigma_1}{\sigma_c} = \left(\frac{M}{B}\frac{\sigma_3}{\sigma_c} + 1\right)^B \qquad (4.7.5a)$$

where

$$M = \frac{1 + \sin\phi}{1 - \sin\phi}$$

The criterion only considers effect strength and hence ϕ is the drained friction angle. B is a strength dependent constant, $1.0 \geq B \geq 0.5$. For soft soil, B approaches to 1.0, the above equation becomes the Mohr-Coulomb criterion as below,

$$\frac{\sigma_1}{\sigma_c} = 1 + \frac{\sigma_3}{\sigma_c}\frac{1 + \sin\phi}{1 - \sin\phi} \qquad (4.7.5b)$$

For rocks, as the strength increases, M increases, but B reduces approaching to 0.5. The equation then becomes a parabolic envelope very similar to that of the Hoek-Brown criterion.

4.8 Time Dependent Characteristics of Rock Materials

4.8.1 Rheologic Properties of Rock Materials

4.8.2 Effect of Loading Rate on Rock Strength

4.8.3 Failure Mechanism of Rock Material under Impact and Shock Loading

4.9 Laboratory Testing of Rock Materials

This section provides method statement of the common rock mechanics tests. International Society for Rock Mechanics (ISRM) suggested methods is freely available from the ISRM website (www.isrm.net). Readers should refer to the ISRM methods for details.

4.9.1 Petrographic Description

Thin section is prepared and examined under petrographic microscope equipped with modal analysis device, e.g., point counter from a grid over the thin section, as shown in Figure 4.9.1a.

Figure 4.9.1a Petrographic analysis.

Petrographic analysis is reported with the form below.

Project: Co-ordinates: Description of sampling point: Thin section No.:				Location: Specimen No.: Date:			
GEOLOGICAL DESCRIPTION				MACROSCOPIC DESCRIPTION			
Rock name: Petrographic classification: Geological formation:				Degree of weathering: Structure (incl. bedding): Discontinuities:			
MINERAL COMPOSITION						GRAIN SIZE DISTRIBUTION	
Major Component	Vol. %	Minor Component	Vol. %	Accessory	Vol. %	Microns	%
QUALITATIVE DESCRIPTION				SIGNIFICANCE FOR ROCK ENGINEERING			
Texture: Fracturing: Alteration: Matrix:							
GENERAL REMARK				MICROGRAPH PHOTO OF TYPICAL FEATURES OF THIN SECTION			

International Society for Rock Mechanics (ISRM), Commission on Testing Methods (1978), Suggested methods for petrographic description of rocks.

4.9.2 Density, Porosity and Water Content

(a) Density of Samples of Regular Shape

The mass of the samples is weighed and its volume is calculated. The bulk density is the mass per unit volume.

(b) Density of Sample of Irregular Shape

The mass of the samples is weighed (M_{bulk}), the rock samples are saturated by water immersion in a vacuum of 600 Pa for more than 1 hour, with periodic agitation to remove trapped air. The samples are then transferred underwater to a basket in an immersion bath. Their saturated-submerged mass M_{sub} is determined from the difference between the saturated-submerged mass of the basket plus sample and that of the basket alone. The samples are then taken out from the immersion bath and surface dried with a moist cloth, their saturated-surface-dry mass M_{sat} is recorded. The bulk volume (V_{bulk}) and bulk density (ρ_{bulk}) are calculated as:

$$V_{bulk} = \frac{(M_{sat} - M_{sub})}{\rho_w}$$

$$\rho_{bulk} = \frac{M_{bulk}}{V_{bulk}}$$

(c) Porosity of Rock Samples

M_{bulk}, M_{sat}, M_{sub} and V_{bulk} are determined using the same method as that for density measurement of rock samples with irregular shape. The samples are dried to a constant mass at a temperature of 105°C in an oven and cooled for 30 min in a desiccator, and the dry mass M_{dry} is measured. Pore volume (V_v) and porosity (n) are calculated by

$$V_v = \frac{(M_{sat} - M_{dry})}{\rho_w}$$

$$n = \frac{V_v}{V_{bulk}} \times 100\%$$

(d) Water Content of Rock Samples

M_{bulk}, and M_{dry} are determined using the same method as that for density and porosity measurement of rock samples with irregular shape. Water content (w) is calculated by

$$w = \frac{(M_{bulk} - M_{dry})}{M_{dry}} \times 100\%$$

Reporting of results includes description of the rocks, precautions taken to retain water during sampling and storage.

International Society for Rock Mechanics (ISRM), Commission on Testing Methods (1977), Suggested methods for determining water content, porosity, density, absorption and related properties and swelling and slake-durability index properties.

4.9.3 Compression Tests

(a) Uniaxial Compression Strength Test

Specimens of right circular cylinders having a height to diameter ratio of 2 or higher are prepared by cutting and grinding. Two axial and one circumferential deformation measurement devices (LVDTs) are attached to each of the specimen. The specimen is then compressed under a stiff compression machine with a spherical seating. The axial stress is applied with a constant strain rate around 1 μm/s such that failure occurs within 5-10 minutes of loading. The load is measured by a load transducer. Load, two axial deformations and one circumferential deformation measurements are recorded at every 2-5 KN interval until failure. Uniaxial compressive strength, Young's modules (at 50% of failure stress) and Poisson's ratio (at 50% of failure stress) can be calculated from the failure load, stress and strain relationship.

Uniaxial compressive strength, σ_c, is calculated as the failure load divided by the initial cross sectional area of the specimen.

Axial tangential Young's modulus at 50% of uniaxial compressive strength, $E_{t50\%}$ is calculated as the slope of tangent line of axial stress - axial strain curve at a stress level equals to 50% of the ultimate uniaxial compressive strength.

Poisson's ratio at 50% of uniaxial compressive strength, $\nu_{50\%}$, is calculated as:

$$\nu_{50\%} = -\frac{\text{slope of axial stress-strain curve at 50\% of } \sigma_c}{\text{slope of lateral stress-strain curve at 50\% of } \sigma_c}$$

Reporting of results includes description of the rock, specimen anisotropy, specimen dimension, density and water content at time of test, mode of failure, uniaxial

compressive strength, modulus of elasticity, Poisson's ratio, stress-strain (axial and lateral) curves to failure.

Figure 4.9.3a A typical uniaxial compression test set-up with load and strain measurements.

(b) Triaxial Compression Strength Test

Specimens of right circular cylinders having a height to diameter ratio of 2 or higher are prepared by cutting and grinding. Two axial and two lateral deformation (or a circumferential deformation if a circumferential chain LVDT device is used), measurement devices are attached to each of the specimen. The specimen is placed in a triaxial cell (e.g., Hoek-Franklin cell) and a desired confining stress is applied and maintained by a hydraulic pump. The specimen is then further compressed under a stiff compression machine with a spherical seating. The axial stress is applied with a constant strain rate around 1 μm/s such that failure occurs within 5-15 minutes of loading. The load is measured by a load transducer. Load, 2 axial strain or deformation and 2 lateral strains or deformation (or a circumferential deformation if a circumferential chain LVDT device is used) are recorded at a fixed interval until failure. Triaxial compressive strength, Young's modules (at 50% of failure stress) and Poisson's ratio (at 50% of failure stress) can be calculated from the axial failure load, stress and strain relationship.

Triaxial compressive strength, σ_1, is calculated as the axial failure load divided by the initial cross sectional area of the specimen.

Axial tangential Young's modulus at 50% of triaxial compressive strength, $E_{t50\%}$ is calculated as the slope of tangent line of axial stress - axial strain curve at a stress level equals to 50% of the ultimate uniaxial compressive strength.

Poisson's ratio at 50% of triaxial compressive strength is calculated with the same methods as for the uniaxial compression test.

For a group of triaxial compression tests at different confining stress level, Mohr's stress circle are plotted using confining stress as σ_3 and axial stress as σ_1. Failure envelopes (Mohr, Coulomb or Hoek and Brown) and parameters of specified failure criterion are determined.

Reporting of results includes description of the rock, specimen anisotropy, specimen dimension, density and water content at time of test, mode of failure, triaxial compressive strength, modulus of elasticity, Poisson's ratio, stress-strain (axial and lateral) curves to failure, Mohr's circles and failure envelope.

Figure 4.9.3b Triaxial compression test using Hoek cell.

International Society for Rock Mechanics (ISRM), Commission on Testing Methods (1979), Suggested methods for determining the uniaxial compressive strength and deformability of rock materials.

International Society for Rock Mechanics (ISRM), Commission on Testing Methods (1999), Suggested methods for complete stress-strain curve for intact rock in uniaxial compression.

International Society for Rock Mechanics (ISRM), Commission on Testing Methods (1978), Suggested methods for determining the strength of rock materials in triaxial compression.

International Society for Rock Mechanics (ISRM), Commission on Testing Methods (1983), Suggested methods for determining the strength of rock materials in triaxial compression: revised version.

4.9.4 Tensile Tests

(a) Direct Tension Test

Direct tension tests on rock materials are not common, due to the difficulty in specimen preparation. For direct tension test, rock specimen is to be prepared in dog-bone shape with a thin middle. The specimen is then loaded in tension by pulling from the two ends.

Deformation modulus can be measured by having strain gauges attached to the specimen. calculation and the Young's modulus and the Poisson's ratio is similar to that for the uniaxial compression test.

(b) Brazilian Tensile Strength Test

Cylindrical specimen of diameter approximately equals to 50 mm and thickness approximately equal to the radius is prepared. The cylindrical surfaces should be free from obvious tool marks and any irregularities across the thickness. End faces shall be flat to within 0.25 mm and square and parallel to within 0.25°. The specimen is wrapped around its periphery with one layer of the masking tape and loaded into the Brazil tensile test apparatus across its diameter. Loading is applied continuously at a constant rate such that failure occurs within 15-30 seconds. Ten specimens of the same sample shall be tested.

The tensile strength of the rock is calculated from failure load (P), specimen diameter (D) and specimen thickness (t) by the following formula:

$$\sigma_t = -\frac{0.636\ P}{}$$

$$\frac{}{D\ t}$$

Reporting of results includes description of the rock, orientation of the axis of loading with respect to specimen anisotropy, water content and degree of saturation, test duration and loading rate, mode of failure.

Figure 4.9.4b Brazilian tensile test.

(c) Flexure Tension Test

International Society for Rock Mechanics (ISRM), Commission on Testing Methods (1978), Suggested methods for determining tensile strength of rock materials.

4.9.5 Shear Strength Tests

(a) Direct Punch Shear

(b) Shear Strength Determination by Triaxial Compression Results

Shear strength parameters, cohesion (c) and international friction angle (ϕ) can be determined from triaxial compression test data.

The Mohr's circle can be plotted for a series of triaxial tests results with σ_1 at different σ_3, forming a series circles, as typically shown in the figure below. A straight line is draw to fit best by tangent to all the Mohr's circles. The line represents the shear strength envelope. The angle of the line to the horizontal is the internal friction angle ϕ, and the intercept at τ axis is the cohesion c.

Alternatively, a series equation can be formed for sets of σ_1 and σ_1, based on the Mohr-Coulomb criterion,

$$\sigma_1 = \frac{2c\cos\phi + \sigma_3 (1 + \sin\phi)]}{1 - \sin\phi}$$

Cohesion c and friction angle ϕ can be computed by solving the equations.

4.9.6 Point Load Strength Index Test

Point load test of rock cores can be conducted diametrically and axially. In diametrical test, rock core specimen of diameter D is loaded between the point load apparatus across its diameter. The length/diameter ratio for the diametrical test should be greater than

1.0. For axial test, rock core is cut to a height between 0.5 D to D and is loaded between the point load apparatus axially. Load at failure is recorded as P. Uncorrected point load strength, I_s, is calculated as:

$$I_s = P / D_e^2$$

where D_e, the "equivalent core diameter", is given by:

$D_e^2 = D^2$ for diametrical test;
$= 4 A / \pi$ for axial, block and lump tests;

$A = H D$ = minimum cross sectional area of a plane through the loading points.

The point load strength is corrected to the point load strength at equivalent core diameter of 50 mm. For $D_e \neq 50$ mm, the size correction factor is:

$$F = (D_e / 50)^{0.45}$$

The corrected point load strength index, $I_{s(50)}$ is calculated as:

$$I_{s(50)} = F I_s$$

Figure 4.9.6a Point load test.

International Society for Rock Mechanics (ISRM), Commission on Testing Methods (1985), Suggested method for determining point load strength.

4.9.7 Ultrasonic wave velocity

Cylindrical rock sample is prepared by cutting and lapping the ends. The length is measured. An ultrasonic digital indicator consist a pulse generator unit, transmitter and receiver transducers are used for sonic pulse velocity measurement. The transmitter and the receiver are positioned at the ends of specimen and the pulse wave travel time is measured. The velocity is calculated from dividing the length of rock sample by wave travel time.

Both P-wave and S-wave velocities can be measured.

Figure 4.9.7a Measuring P and S wave velocity in a rock specimen.

International Society for Rock Mechanics (ISRM), Commission on Testing Methods (1978), Suggested methods for determining sound velocity.

4.9.8 Hardness

(a) Schmidt Hammer Rebound Hardness

A Schmidt hammer with rebound measurement is used for this test. The Schmidt hammer is point perpendicularly and touch the surface of rock. The hammer is released and reading on the hammer is taken. The reading gives directly the Schmidt hammer hardness value. The standard Schmidt hardness number is taken when the hammer is point vertically down. If the hammer is point to horizontal and upward, correction is needed to add to the number from the hammer. The correction number is given in Table 4.9.8a.

Table 4.9.8a Correction number for Schmidt hammer with inclination angle

Rebound Number	Vertically downward	45° downward	Horizontal	45° upward	Vertically upward
10	0	–0.8			–3.2
20	0	–0.9	–8.8	–6.9	–3.4
30	0	–0.8	–7.8	–6.2	–3.1
40	0	–0.7	–6.6	–5.3	–2.7
50	0	–0.6	–5.3	–4.3	–2.2
60	0	–0.4	–4.0	–3.3	–1.7

At least 20 tests should be conducted on any one rock specimen. It is suggest to omit 2 lowest and 2 highest reading, and to use the remaining reading for calculating the average hardness value.

Report of results should include descriptions of rock type, location, size and shape, and orientation of hammer axis.

Figure 4.9.8a Schmidt hammer rebound hardness test.

(b) Shore Hardness

International Society for Rock Mechanics (ISRM), Commission on Testing Methods (1978), Suggested methods for determining hardness and abrasiveness of rocks.

International Society for Rock Mechanics (ISRM), Commission on Testing Methods (2006), Suggested methods for determining the shore hardness value for rock.

4.9.9 Fracture Toughness

(a) Cracked Cheron Notched Brazilian Disc (CCNBD)

Figure 4.9.9a CCNBD fracture toughness test set-up-

(b) Chevron Bend Specimen

(c) Short Rod Specimen

International Society for Rock Mechanics (ISRM), Commission on Testing Methods (1988), Suggested methods for determining the fracture toughness of rock.

International Society for Rock Mechanics (ISRM), Commission on Testing Methods (1995), Suggested methods for determining Mode I fracture toughness using cracked Cheron notched Brazilian disc (CCNBD) specimens.

4.9.10 Abrasivity

(a) Cerchar Abrasivity Test

The Cerchar abrasivity test is an abrasive wear with pressure test . It was proposed by the Laboratoire du Centre d'Etudes et Recherches des Charbonnages (Cerchar) in France. The testing apparatus is featured in Figure 4.9.10a. It consists of a vice for holding rock sample (1), which can be moved across the base of the apparatus by a handwheel (2), that drives a screwthread of pitch 1 mm/revolution turning. Displacement of the vice (1) is measured by a scale (3). A steel stylus (4), fitting into a holder (5), loaded on the surface of the rock sample. A dead weight (6) of 70 N is applied on the stylus.

Figure 4.9.10a Cerchar abrasivity test West apparatus (West 1989).

To determine the CAI value the rock is slowly displaced by 10 mm with a velocity of approximately 1 mm/s. The abrasiveness of the rock is then obtained by measuring the resulting wear flat on the tip of the steel stylus. The CAI value is calculated as,

$CAI = 10^{-2}\ d$

where d is the wear flat diameter of the stylus tip in μm.

(b) NTNU Abrasion Test

West G (1989), Rock abrasiveness testing for tunnelling. International Journal of Rock Mechanics and Mining Sciences, Vol.26, pp.151-160.

4.9.11 Indentation Test

4.9.12 Slake Durability Test

Select representative rock sample consisting of 10 lumps each of 40-60g, roughly spherical in shape with corners rounded during preparation. The sample is placed in the test drum of 2 mm standard mesh cylinder of 100 mm long and 140 mm in diameter with solid removable lid and fixed base, and is dried to a constant mass at 105°C. The mass of drum and sample is recorded (Mass A). The sample and drum is placed in trough which is filled with slaking fluid, usually tap water at 20°C, to a level 20 mm below the drum axis, and the drum is rotated at 20 rpm for 10 minutes (Figure 4.9.12a). The drum and sample are removed from trough and oven dried to a constant mass at 105°C without the lid. The mass of the drum and sample is recorded after cooling (Mass B). The slaking and drying process is repeated and the mass of the drum and sample is recorded (Mass C). The drum is brushed clean and its mass is recorded (Mass D).

Figure 4.9.12a Slake durability test.

The slake-durability index is taken as the percentage ratio of final to initial dry sample masses after to cycles,

$$\text{Slake-durability index, } I_{d2} = \frac{C - D}{A - D} \times 100\%$$

The first cycle slake-durability index should be calculated when I_{d2} is 0-10%,

$$\text{Slake-durability index, } I_{d1} = \frac{B - D}{A - D} \times 100\%$$

Table 4.9.12a Slake Durability Classification

Slake Durability Index I_{d2} (%)	Classification
0 – 25	Very low
25 – 50	Low
50 – 75	Medium
75 – 90	High
90 – 95	Very high
95 – 100	Extremely high

International Society for Rock Mechanics (ISRM), Commission on Testing Methods (1977), Suggested methods for determining water content, porosity, density, absorption and related properties and swelling and slake-durability index properties.

4.9.13 Swelling

(a) Unconfined Swelling Test

Prepared rock specimen of 30-50 mm high is placed in a swelling cell (Figure 4.9.13a). Micrometer dial gauges reading to 0.002 mm, mounted to measure the swelling displacements of the specimen in three perpendicular directions. The cell is then flooded with water to cover the specimen, and the swelling displacements recorded as a function of time elapsed, until they reach constant levels or pass peaks. The swelling strains are calculated as

ε_{swell} = (maximum swelling displacement / initial length) × 100%

in their respective directions.

Figure 4.9.13a Unconfined swelling test.

(b) Confined Swelling Test

Figure 4.9.13b Confined axial swelling test.

International Society for Rock Mechanics (ISRM), Commission on Testing Methods (1977), Suggested methods for determining water content, porosity, density, absorption and related properties and swelling and slake-durability index properties.

Further Readings

Jaeger JC, Cook NGW, Fundamentals of Rock Mechanics, 3rd Edition. Chapman and Hall, London, 1979.

Brady BHG, Brown ET, Rock Mechanics for Mining Engineers, 2nd Edition.

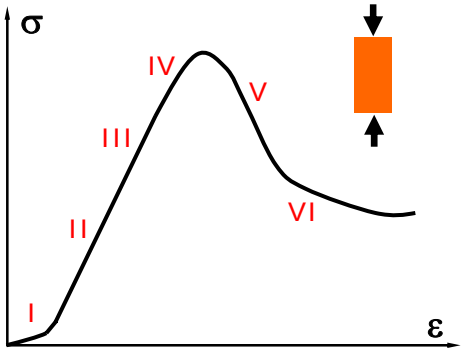
σ
IV
V
III
VI
II
I
ε

4.2.1a

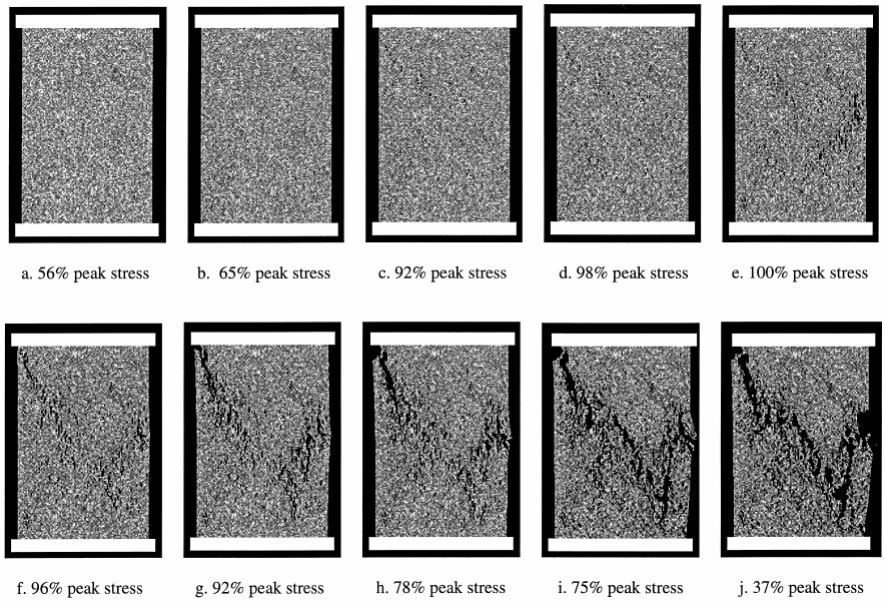
a. 56% peak stress
b. 65% peak stress
c. 92% peak stress
d. 98% peak stress
e. 100% peak stress
f. 96% peak stress
g. 92% peak stress
h. 78% peak stress
i. 75% peak stress
j. 37% peak stress

4.2.1b

Around peak stress (IV-V)

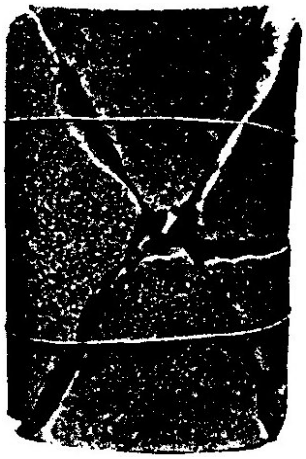

Post peak stress (VI)

4.2.1c

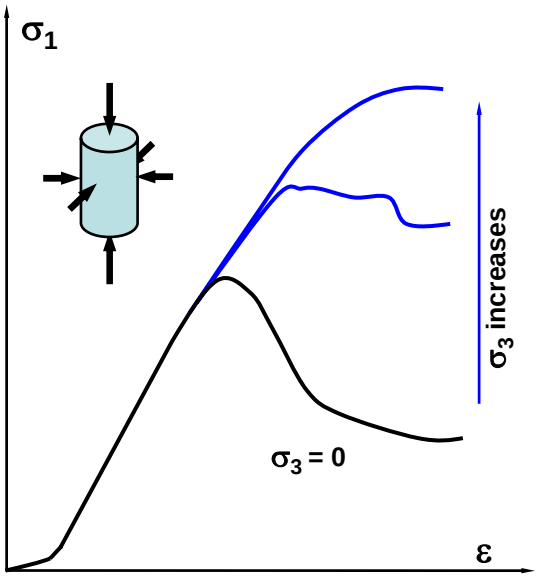

4.2.1d

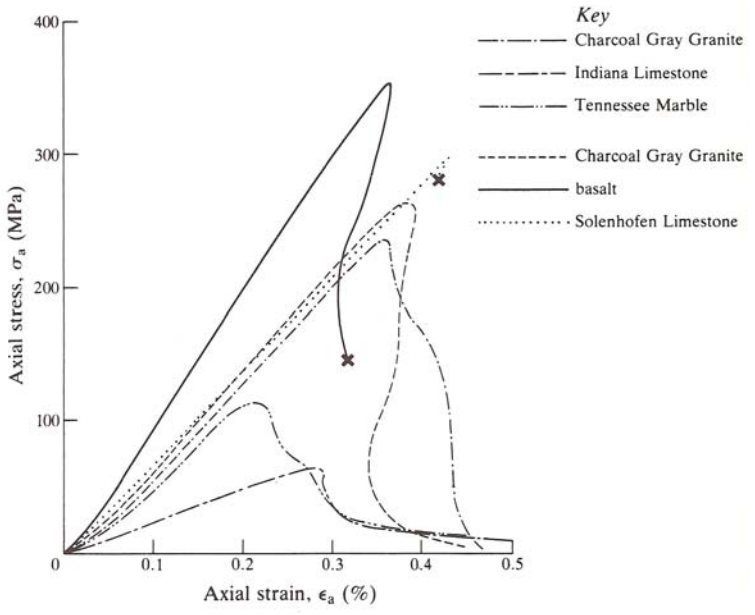
Key
Charcoal Gray Granite
Indiana Limestone
Tennessee Marble
Charcoal Gray Granite
basalt
Solenhofen Limestone
Axial stress, σ_a (MPa)
400
300
200
100
0
0.1
0.2
0.3
0.4
0.5
Axial strain, ϵ_a (%)

4.2.3a

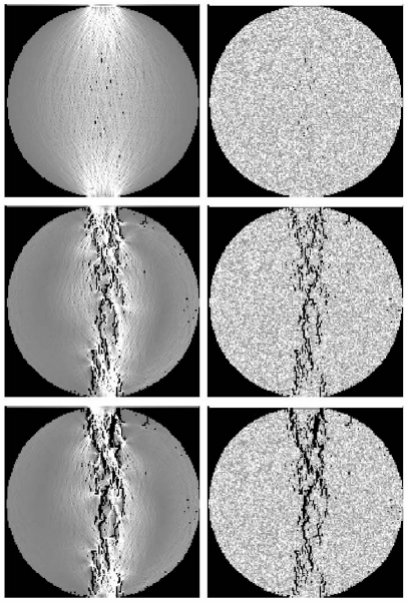

4.2.4a

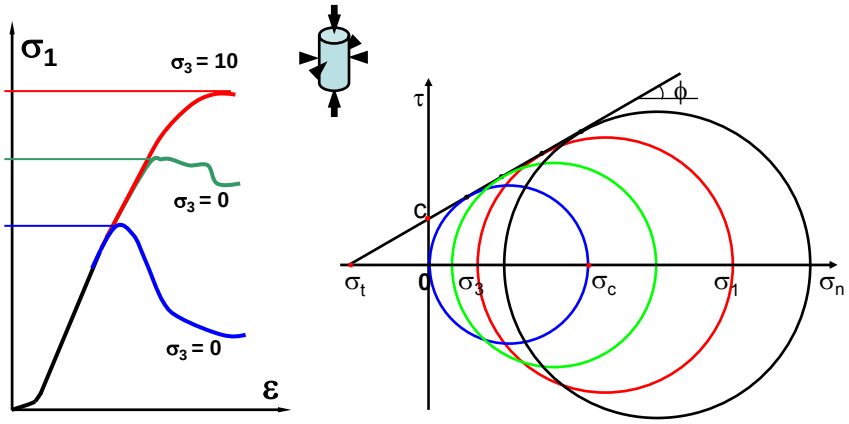
σ1
σ3 = 10
σ3 = 0
σ3 = 0
ε
τ
c
ϕ
σt
0
σ3
σc
σ1
σn

4.2.5a

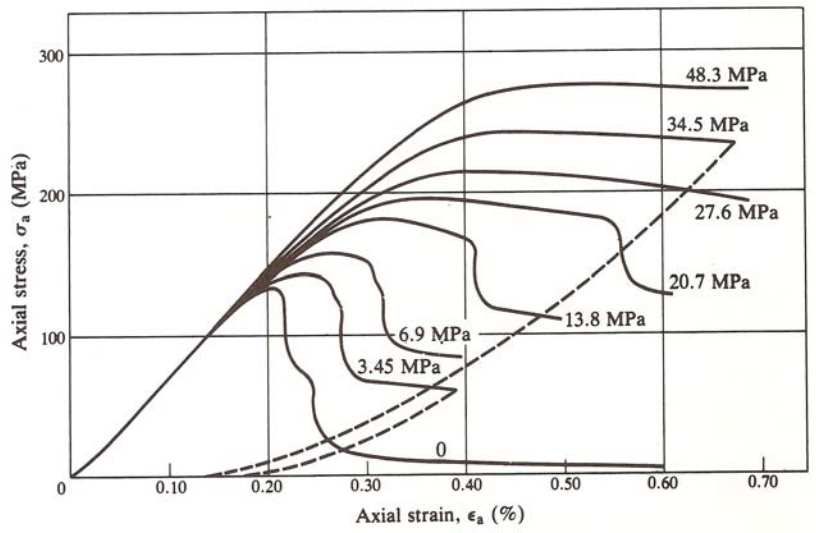
300
200
100
0
Axial stress, σa (MPa)
48.3 MPa
34.5 MPa
27.6 MPa
20.7 MPa
13.8 MPa
6.9 MPa
3.45 MPa
0
0.10
0.20
0.30
0.40
0.50
0.60
0.70
Axial strain, εa (%)

4.3.1a

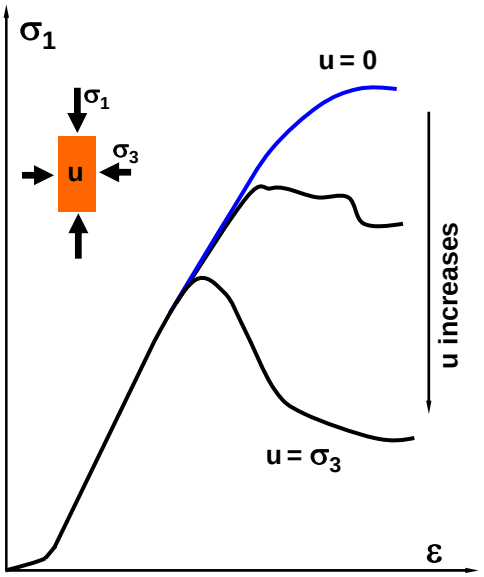
σ1
u = 0
σ1
σ3
u
u increases
u = σ3
ε

4.3.2a

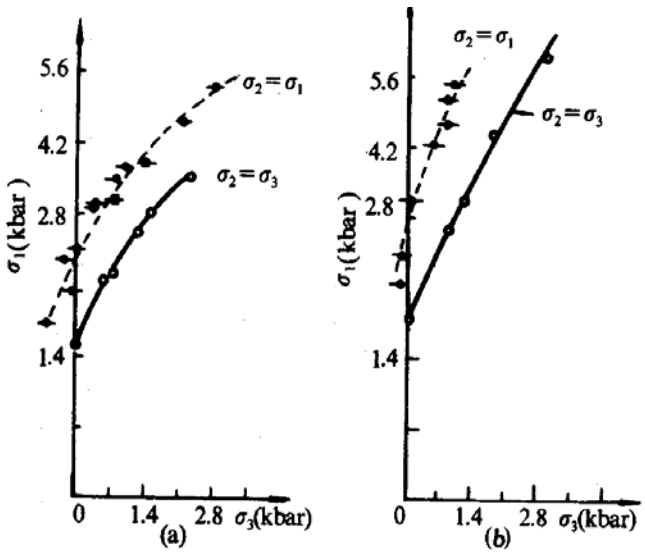
5.6
4.2
2.8
1.4
σ1(kbar)
σ2=σ1
σ2=σ3
0
1.4
2.8
σ3(kbar)
(a)
σ2=σ1
σ2=σ3
(b)

4.3.3a

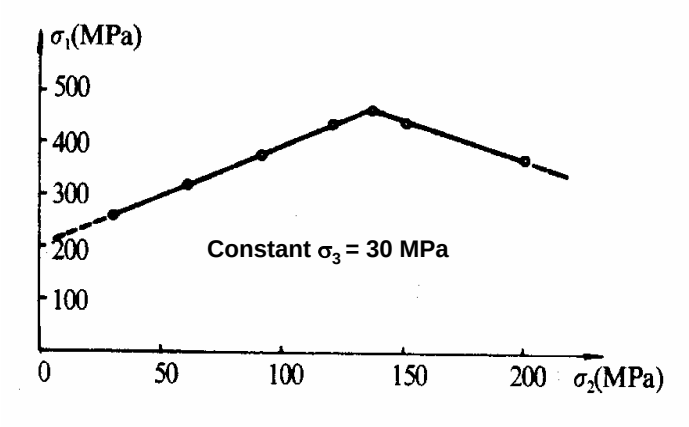
σ_1(MPa)
500
400
300
200
100
0
50
100
150
200
σ_2(MPa)
Constant σ_3 = 30 MPa

4.3.3b

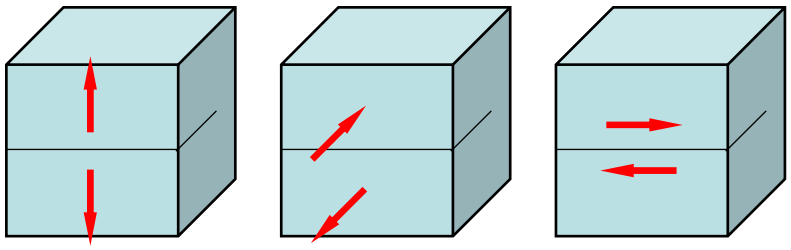
Mode I
Mode II
Mode III

4.4.2a

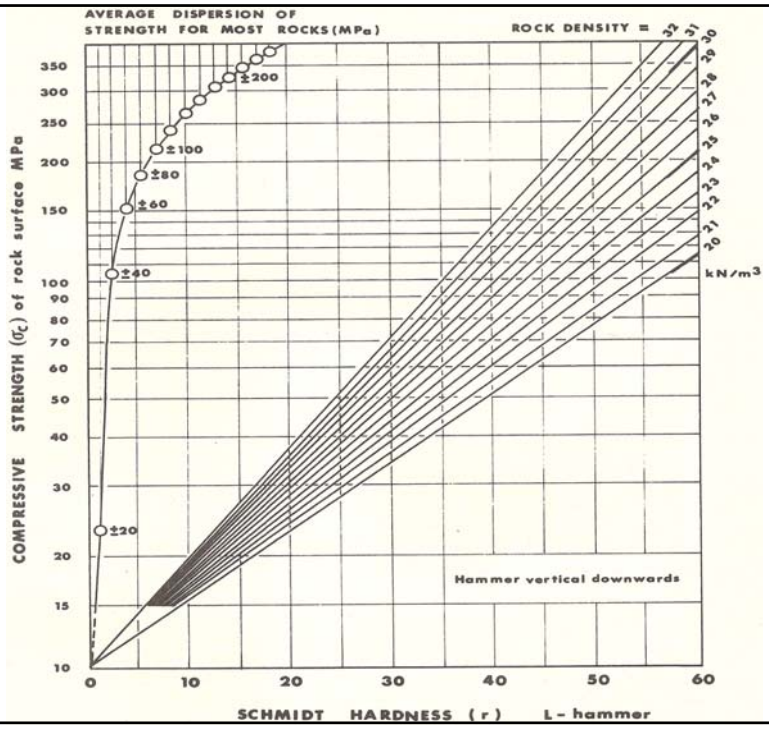
AVERAGE DISPERSION OF
STRENGTH FOR MOST ROCKS (MPa)
ROCK DENSITY =
COMPRESSIVE STRENGTH (σ_c) of rock surface MPa
±200
±100
±80
±60
±40
±20
kN/m3
Hammer vertical downwards
SCHMIDT HARDNESS (r) L-hammer

4.5.1a

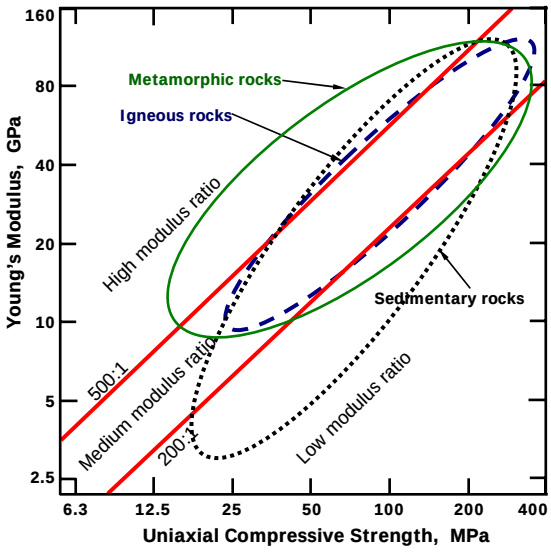
Metamorphic rocks
Igneous rocks
High modulus ratio
Sedimentary rocks
500:1
Medium modulus ratio
200:1
Low modulus ratio
Young's Modulus, GPa
Uniaxial Compressive Strength, MPa

4.5.4a

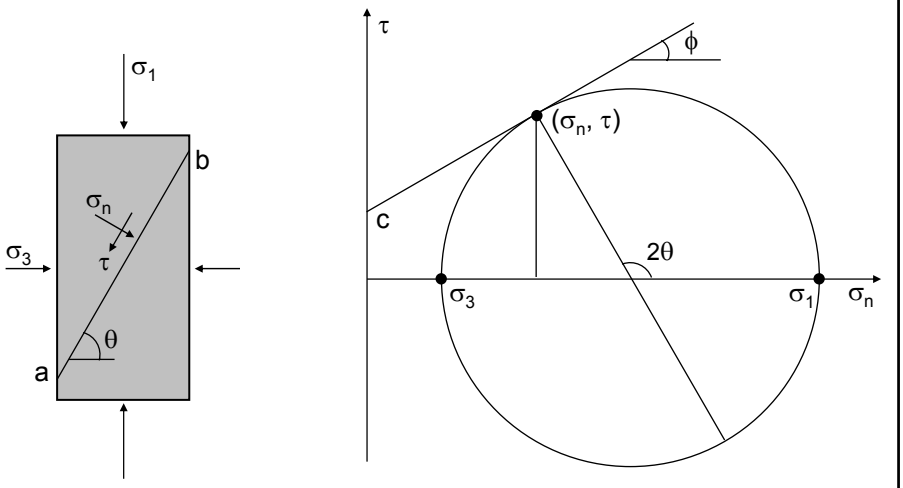
σ1
b
σn
σ3
τ
θ
a
τ
ϕ
(σn, τ)
c
2θ
σ3
σ1
σn

4.6.1a

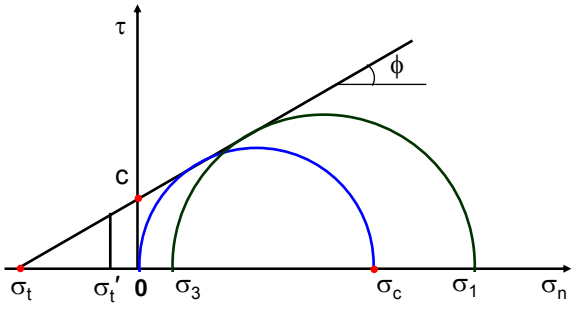
τ
ϕ
c
σt
σt′
0
σ3
σc
σ1
σn

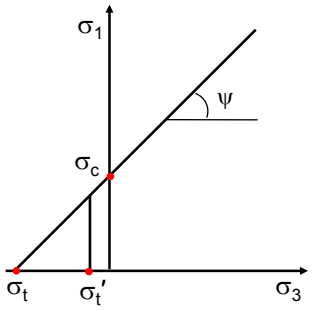
σ1
ψ
σc
σt
σt′
σ3

4.6.1b

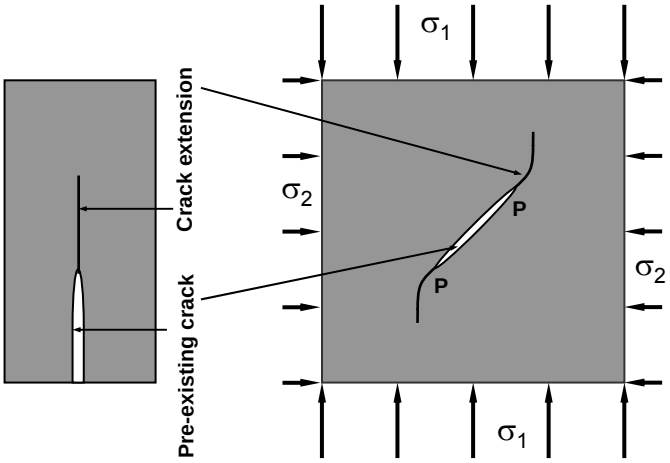
σ1
Crack extension
σ2
P
P
σ2
Pre-existing crack
σ1

4.6.2a

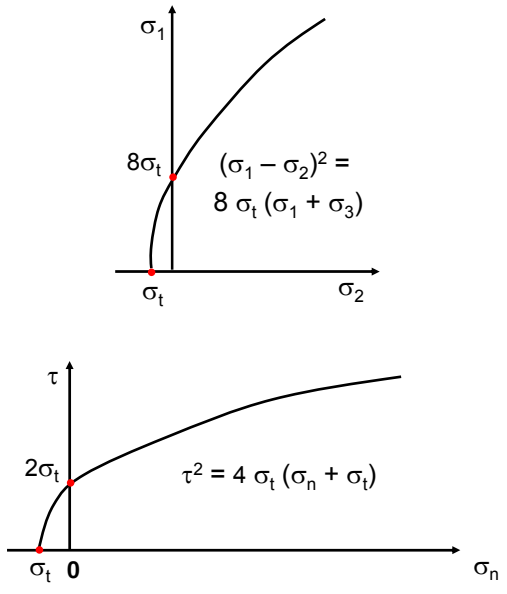
σ1
8σt
(σ1 – σ2)2 =
8 σt (σ1 + σ3)
σt
σ2
τ
2σt
τ2 = 4 σt (σn + σt)
σt 0
σn

4.6.2b

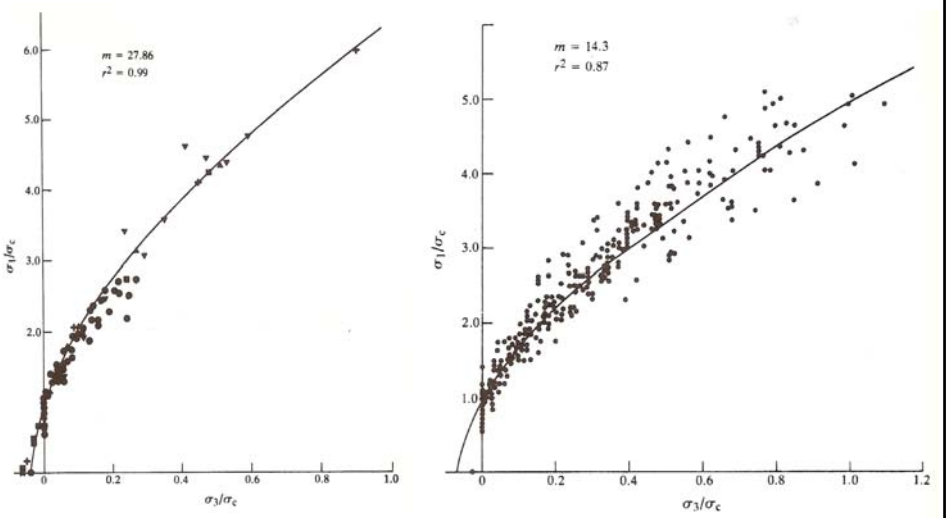
m = 27.86
r² = 0.99
σ1/σc
σ3/σc
m = 14.3
r² = 0.87
σ1/σc
σ3/σc

4.6.3a

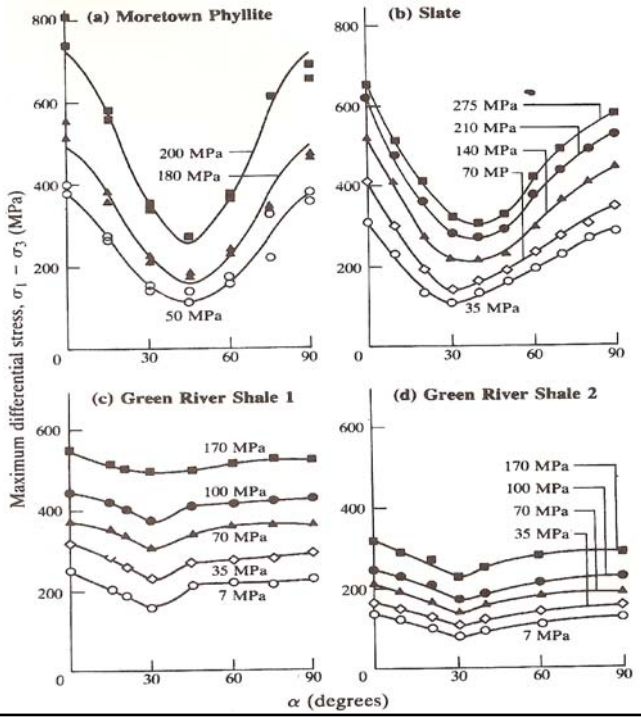
(a) Moretown Phyllite
200 MPa
180 MPa
50 MPa
(b) Slate
275 MPa
210 MPa
140 MPa
70 MP
35 MPa
(c) Green River Shale 1
170 MPa
100 MPa
70 MPa
35 MPa
7 MPa
(d) Green River Shale 2
170 MPa
100 MPa
70 MPa
35 MPa
7 MPa
Maximum differential stress, σ1 − σ3 (MPa)
α (degrees)

4.7.1a

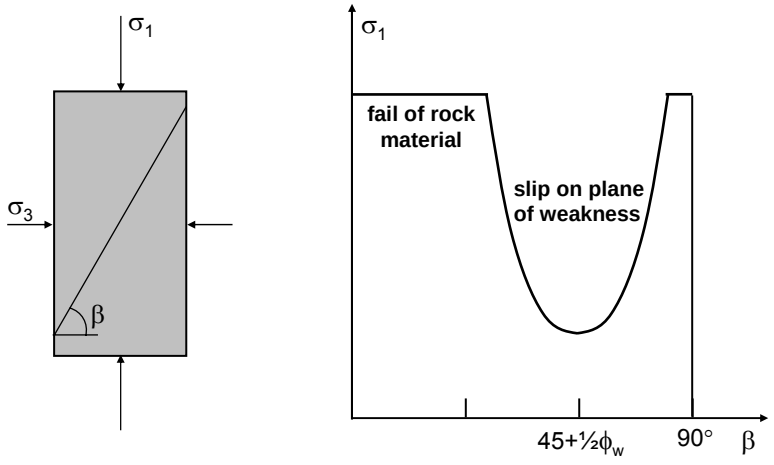
σ1
σ3
β
σ1
fail of rock material
slip on plane of weakness
45+½φw
90°
β

4.7.1b

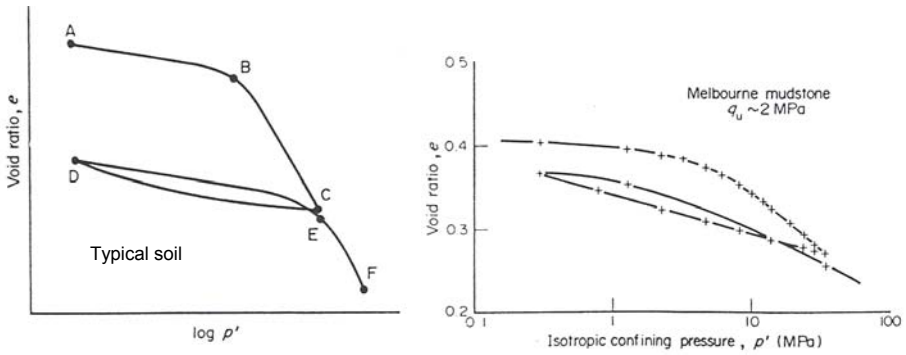
A
B
C
D
E
F
Void ratio, e
log p'
Typical soil
Melbourne mudstone
qu ~2 MPa
Void ratio, e
0.5
0.4
0.3
0.2
0.1
1
10
100
Isotropic confining pressure, p' (MPa)

4.7.5a

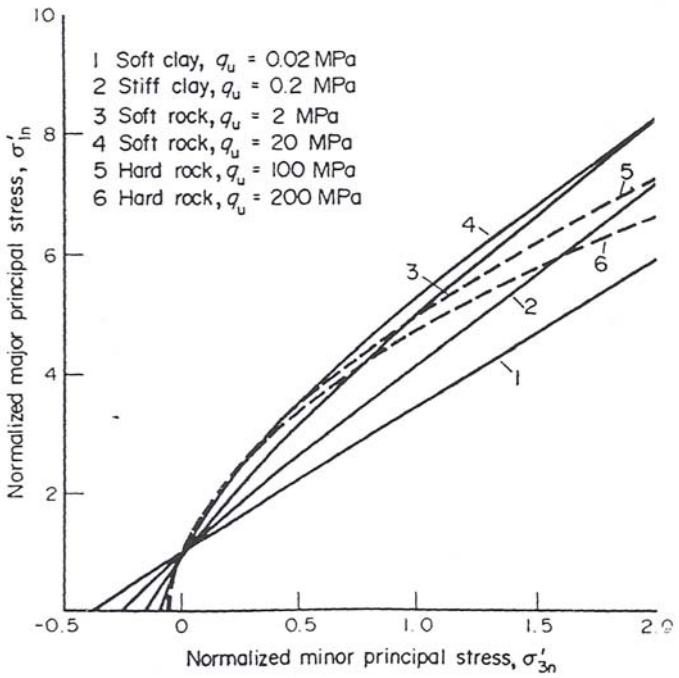
1 Soft clay, q_u = 0.02 MPa
2 Stiff clay, q_u = 0.2 MPa
3 Soft rock, q_u = 2 MPa
4 Soft rock, q_u = 20 MPa
5 Hard rock, q_u = 100 MPa
6 Hard rock, q_u = 200 MPa
Normalized major principal stress, σ'_{1n}
Normalized minor principal stress, σ'_{3n}
10
8
6
4
2
-0.5
0
0.5
1.0
1.5
2.0

4.7.5b

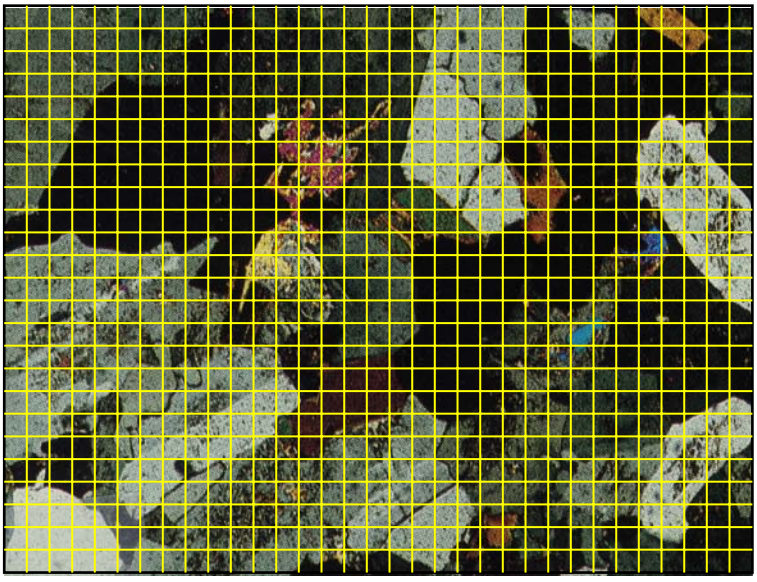

4.9.1a

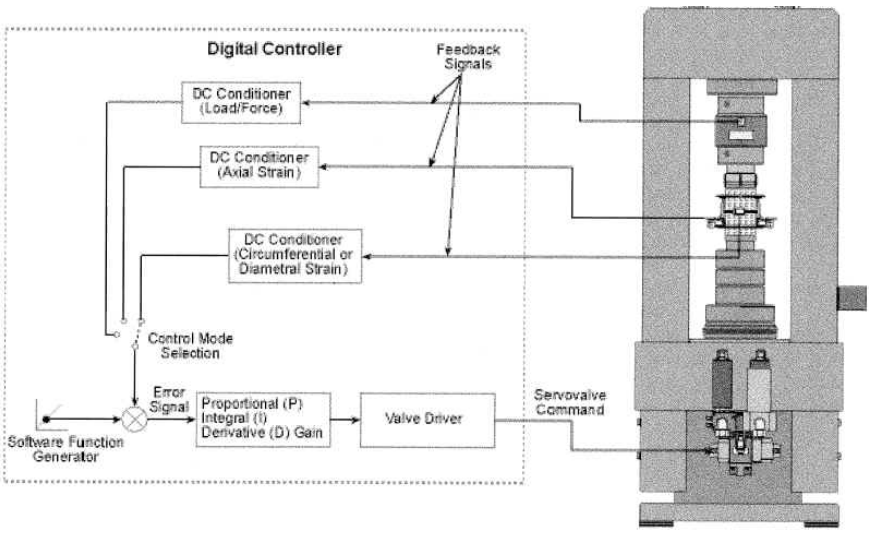

4.9.3a

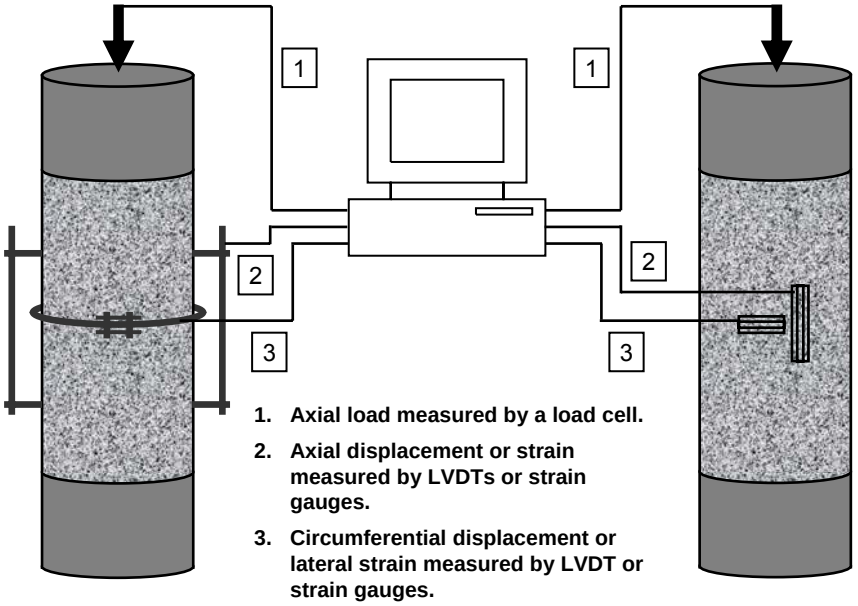

1. **Axial load measured by a load cell.**
2. **Axial displacement or strain measured by LVDTs or strain gauges.**
3. **Circumferential displacement or lateral strain measured by LVDT or strain gauges.**

4.9.3a

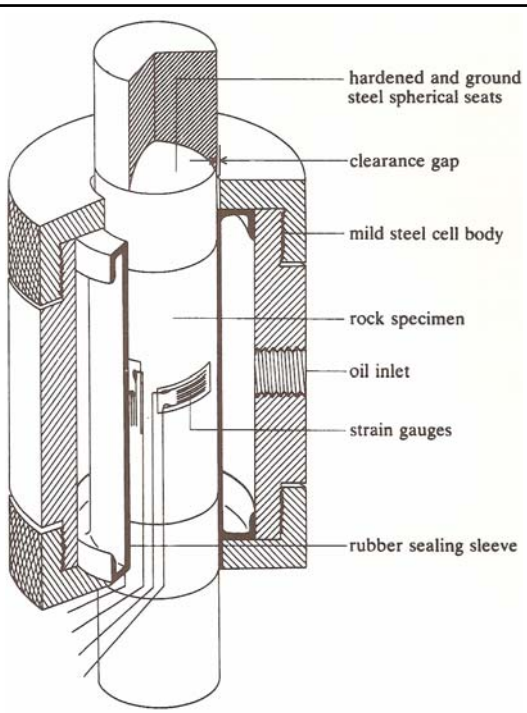
hardened and ground steel spherical seats
clearance gap
mild steel cell body
rock specimen
oil inlet
strain gauges
rubber sealing sleeve

4.9.3b

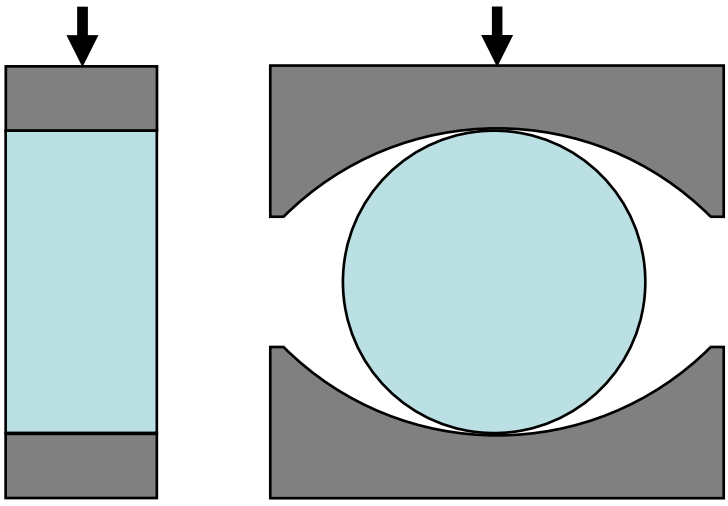

4.9.4b

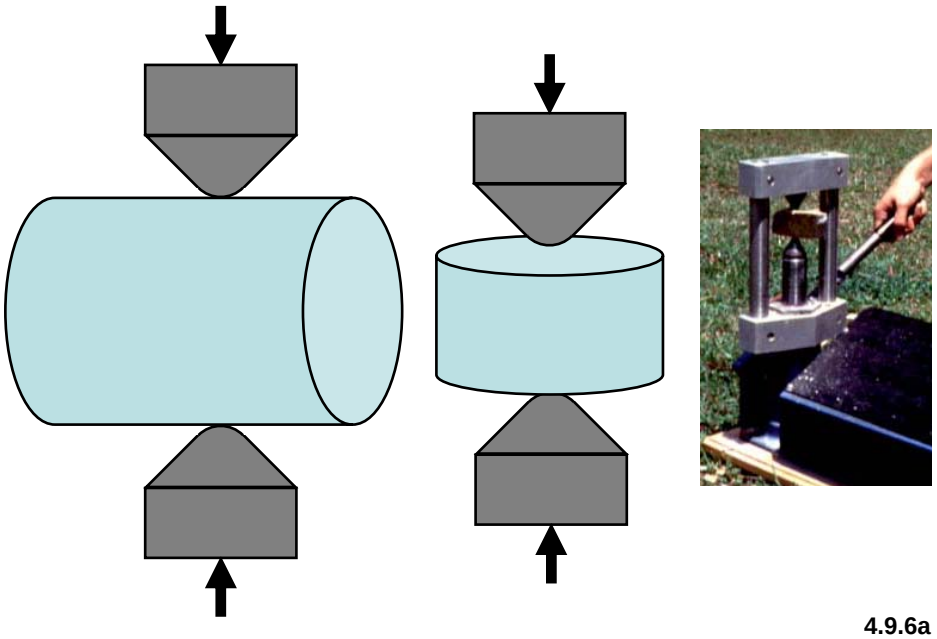

4.9.6a

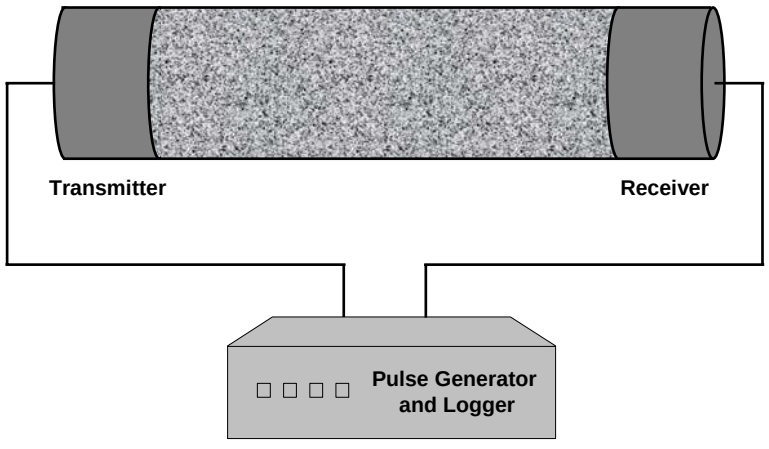

4.9.7a

4.9.8a

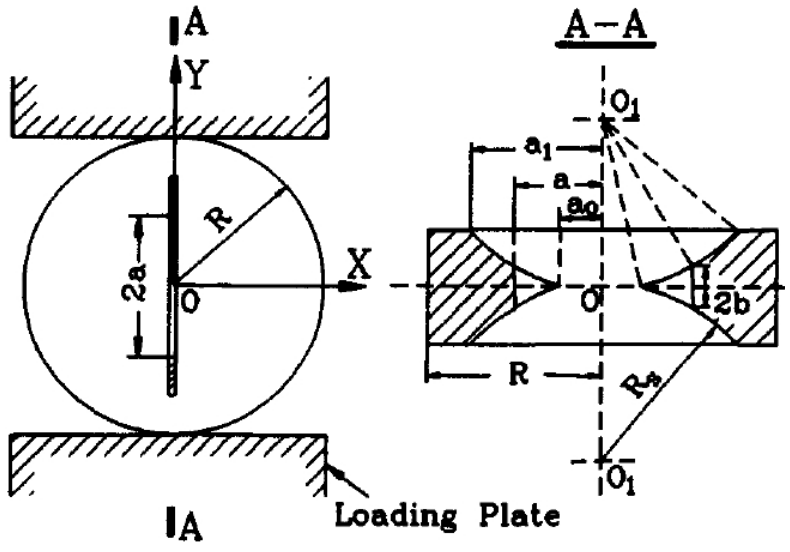

4.9.9a

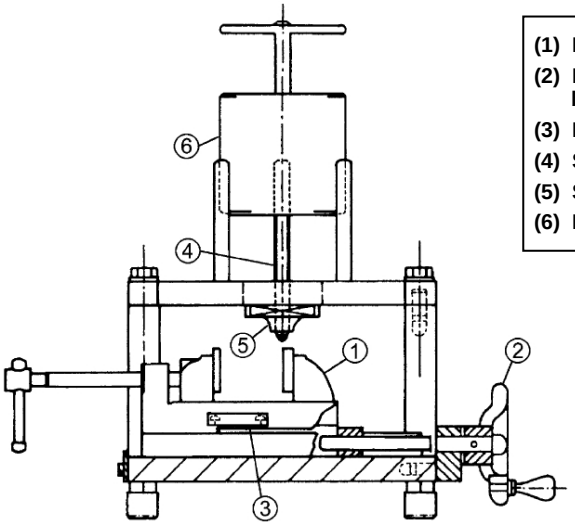

(1) Rock sample holder.
(2) Hand wheel for base movement.
(3) Displacement scale.
(4) Steel stylus.
(5) Stylus holder.
(6) Dead weight.

4.9.10a

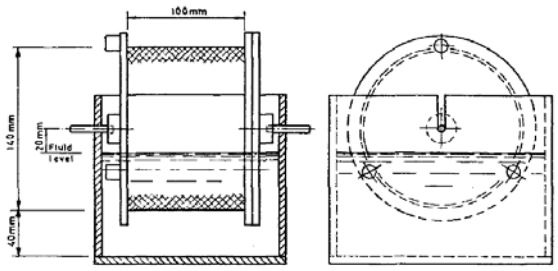

4.9.12a

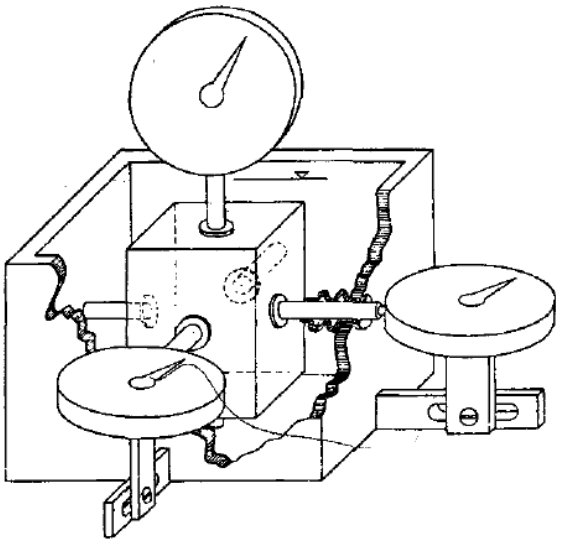

4.9.13a

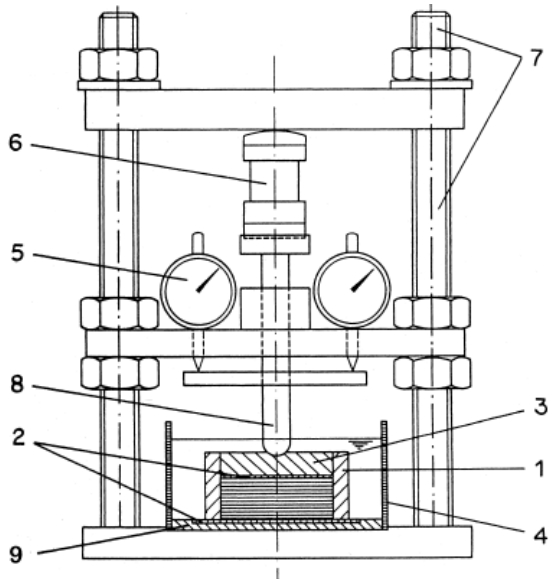

(1) Steel ring.
(2) Porous metal plate.
(3) Steel loading plate.
(4) Container.
(5) Dial gauges.
(6) Load measuring device.
(7) Frame.
(8) Loading piston.
(9) Steel plate.

4.9.13b